■ 1490

Modelling Optical Waveguide Bends by the Method of Lines

Ary Syahriar*[1], Nabil Rayhan Syahriar[2], Jusman Syafiie Djamal[3]
[1,3] Electrical Engineering Department, Faculty of Science and Technology University al Azhar Indonesia,
Jakarta Indonesia
[2] Mechanical Engineering Department, Bandung Institute of Technology
*Corresponding author, e-mail: ary@uai.ac.id

Abstract

A rigorous analytical and semi analytical method of lines has been used to calculate the transverse-electric field attenuation coefficient of guided mode as it travels in waveguide bends structure. Both approaches then were compared to get a better understanding on how the attenuation behaves along single curve waveguides with constant radius of curvature. The Helmholtz Equation in polar coordinate was transformed into a curvalinier coordinate to simulate the waveguide bends using the method of line analysis. The simple absorption boundary conditions are used into the method of lines to demonstrate evanescent field of the guided mode nature as its travels in waveguide bends structures. The results show that a reasonable agreement between both theoretical approaches.

Keywords: Optical waveguide bends, Method of lines, The transverse-electric field attenuation coefficient

1. Introduction

One of the most important optical integrated devices building blocks is waveguide bends because it defines the overall size of integrated optics in single subtrates. Waveguide bends are required in many basic optical structures, including directional couplers, modulators, ring resonators [1], arrayed waveguide filters [2], optical delay lines [3], S-bend attenuators [4]. and Mach-Zehnder interferometers. However, waveguide bends experience loss as the guided mode enters the curved section which depends on confinement factors and radius of curvature. The loss can be minimized by increasing the mode confinement i.e. by increasing the refractive index differences between core and cladding layers or by decreasing radius of curvatures. Increasing mode confinement will increase the coupling losses when waveguide is coupled into the fiber optics and decreasing radius of curvature will increase the overall integrated optics size. In a silica-based waveguide, there is normally only a very slight variation in refractive index across the cross-section, to allow low loss coupling to a single mode fibre. The slight variation in index is most helpful as it permits the vector wave equation to be replaced by a scalar equation in which the electric field is represented by one vector component. This simplification is known as the weak-guidance approximation. Therefore a precise knowledge on bend waveguides characteristics become important to design a compact integrated optical systems.

So far, a number of efficient numerical techniques have been proposed for the analysis of optical waveguides. These include the finite difference method (FDM), the finite element method (FEM), the beam propagation method (BPM), and the method of lines (MoL) [5]. The finite difference method is the oldest numerical method for solving partial differential equations. It is simple to program and easily applied to non-homogenous refractive index profiles. This method subdivides the domain into many subregions, in which the partial derivatives are replaced by finite difference operators. A set of linear equations are then solved to obtain the eigenvalues. The drawback of the FDM is it offers less flexibility in the modeling of the domain since the subregion is normally rectangular in shape [6]. The finite element method (FEM) can model the most intricate domain geometries. In FEM, the waveguide cross section is divided into surface or volume elements and the field in each element is approximated by a polynomial. The field continuity conditions are imposed on all interfaces between the different elements. A variational expression for Maxwell's equations then is employed to obtain an eigenvalue matrix equation which is solved by standard methods. This method requires a more complex

programming structure and is more demanding in both computer time and memory [7]. The beam propagation method (BPM) has been used to analyze various two- and three-dimensional optical devices. The original BPM used an FFT algorithm and solved a paraxial scalar wave equation. The basic idea of the BPM is to represent the electromagnetic field by a superposition of plane waves propagating in homogenous media. The advantages of the BPM are that it can be applied to a structure with an arbitrary cross-section, and that both guided and radiative waves are included in the analysis. However since the formulation is derived under the assumption that the refractive index variation in the transverse direction is very small, the FFT-BPM cannot be applied to structures with large index discontinuities [6].

The method of lines (MoL) has been proved to be a very useful tool for the analysis of general waveguide systems [8]. It is a semi analytical method, in which the wave equation is discretized as far as necessary in the transverse direction and solved analytically in the longitudinal direction, which results in less computational effort. An accurate result can be obtained since the MoL behaves in a stationary fashion and convergence is monotonic [9]. Discontinuous fields can be described accurately because the interface conditions are included in the calculation. Furthermore, the MoL is relatively easy to implement using computer numerical methods. In this paper we compare two different approaches, namely a simple quasi-analytic theory based on integration of a phenomenological absorption coefficient, and the method of lines (MoL). Both are applied to a number of different waveguide bend curvatures.

In this paper we applied the method of lines with third order absorbing boundary condition to analyse weakly guiding optical waveguides bends characteristics. For the first approximation we have transformed the Helmholtz wave equation in polar co-ordinates to Cartesian coordinates to simplify the discretisation of waveguide structures. In the process we compared the results with analytical methods as the correct references that has been developed previously. We found that the MoL results are in good agreement with analytical methods. The discrepencies arised from differents radius of curvature used in the calculation and the choices of absorbing boundaries parameters.

2. Research Method
2.1. Analytical Approach

To analyse the effect of a waveguide bend, consider a bend formed by a circular arc with radius of curvature *r* as shown in Figure 1. It is assumed that only the fundamental mode propagates in the guide. If the radius of curvature is large enough ($r \rightarrow \infty$), then the properties of the mode are effectively those of a mode traveling in a straight guide. However, as *r* decreases, attenuation is expected to occur. Let *P(s)* be the total power carried by the mode at any point *s* along the bend. Assuming that the rate of power loss is proportional to the power carried by the mode at that point, we can write:
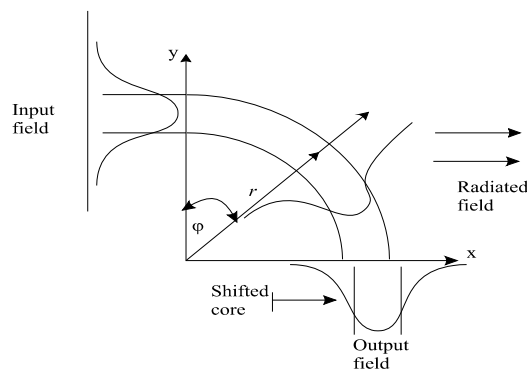

Figure 1. Section of a curved planar waveguide

$$\frac{dP(s)}{ds} = -\alpha P(s) \qquad (1)$$

where α is the attenuation coefficient. Provided α is constant, equation 1 has the solution:

$$P(s) = P(0)e^{-\alpha s} \tag{2}$$

Marcatili and Miller have shown that the attenuation coefficient is indeed constant for a fixed radius, and can be expressed as [10]:

$$\alpha = C_1 e^{-C_2 r} \tag{3}$$

where C_1 and C_2 are functions of the waveguide parameters but are independent of r. Equation 3 shows that the attenuation coefficient increases exponentially with decreasing bending radius; however, if the radius of curvature become large enough the attenuation becomes negligible. It also shows that the change of α with r is dominated by the value of C_2, which (for a weakly-guiding guide) is given by [11]:

$$C_2 = \frac{2\pi}{\lambda} \frac{(2\Delta n_{eff})^{\frac{3}{2}}}{\sqrt{n_2}} \tag{4}$$

Here $\Delta n_{eff} = n_{eff} - n_2$, where n_2 is the refractive index of the cladding.

The C_2 value also provides a method for characterising mode confinement, which is useful when investigating techniques for reducing bend losses. Equation 3 shows that α is also affected (but less strongly) by the value of the coefficient C_1, which is defined as [11]:

$$C_1 = \frac{1}{2Z_c} \frac{\chi_l'}{\chi_t} \tag{5}$$

where the parameters Z_c, χ_t, and χ_l' are given by:

$$Z_c = \frac{n_2}{2\lambda} \left[h + 2\sigma \cos(\frac{\kappa h}{2}) \right]^2 \tag{6}$$

$$\chi_t = \frac{h}{2} + \frac{1}{2\kappa} \sin(\kappa h) + \sigma \cos^2(\frac{\kappa h}{2}) \tag{7}$$

and,

$$\chi_l' = \frac{\sigma}{2} \cos^2 \left[\frac{\kappa h}{2} \right] e^{\frac{h}{\sigma}} \tag{8}$$

where σ is given by:

$$\frac{1}{\sigma} = \sqrt{\beta^2 - k_0 n_2^2} \tag{9}$$

and h, γ and κ have their usual meanings [12].

The C_1 coefficient as defined in equation 4 is not a direct function of Δn_{eff}, but is related to the difference between the propagation constant within the guide and the cladding refractive index n_2. Additionally, the C_1 coefficient is strongly model dependent, and so can be used to calculate the guide shape and other parameters. The above formulation of the C_1 and the C_2 coefficients was based on the derivation made by Marcatili et.al [10] and later adopted by Minford et.al [11]. However, two other formulations have been provided by Lee [12] and Marcuse [13,14]. Lee's version of the C_1 and the C_2 coefficients is as follows [12]:

$$C_1 = \frac{2\gamma^2}{k_o n_2 (\gamma h + 2)} \cos^2(\frac{\kappa h}{2}) e^{\gamma h} \tag{10}$$

and,

$$C_2 = \frac{2\gamma(n_{eff} - n_2)}{n_2} \tag{11}$$

Here, k_o, κ, γ, and h have their usual meaning. In a similar way, Marcuse's version of the coefficients is as follows [14]:

$$C_1 = \frac{2\gamma^2}{\beta(2 + \gamma h)} \frac{\kappa^2}{(n_1^2 - n_2^2)k_o^2} \exp(\gamma h) \tag{12}$$

and,

$$C_2 = \frac{2}{3} \frac{\gamma^3}{\beta^2} \tag{13}$$

here, the propagation constant is defined as $\beta = k_o n_{eff}$. It might be expected that these different formulations would give similar results; however, this was not found to be the case.

2.2. Method of Lines

In this analysis we begin by considering the behaviour of a guided mode as it travels around a bend of constant curvature. Figure 2 shows a schematic of the geometry. The waveguide has a constant radius of curvature r, which is measured from the centre of the guide. The guide is of width h, which is assumed to be much less than r and is centred on a computational window of width w. The core and cladding refractive indices are given by n_1 and n_2 respectively.
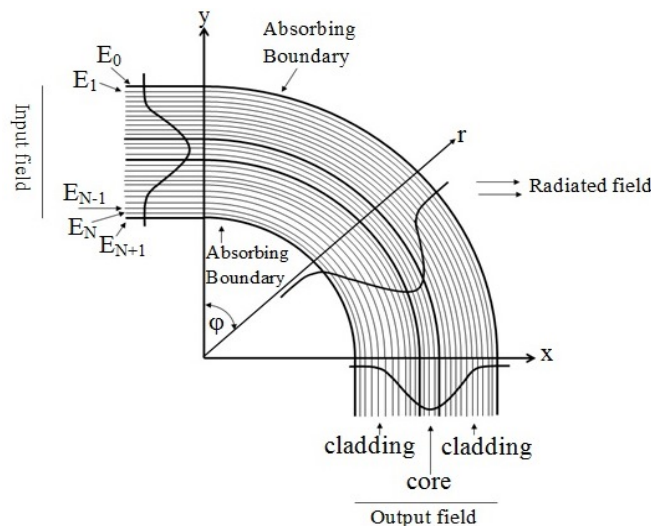

Figure 2. Discretisation of a planar waveguides bends by the MoL

Assuming a y-polarised electric field, the Helmholtz wave equation can be written in polar co-ordinates as [15]:

$$\frac{1}{\rho}\frac{\partial E_y}{\partial \rho} + \frac{\partial^2 E_y}{\partial \rho^2} + \frac{1}{\rho^2}\frac{\partial^2 E_y}{\partial \varphi^2} + k_o^2 n^2 E_y = 0 \tag{14}$$

To implement a numerical solution of equation 14 a modification must be made. It involves changing the co-ordinates to a local co-ordinate system that follows the centre of the waveguide along the propagation direction [15]. This change also allows the possibility of analysing the field profile at the local cross-section. By making the substitution:

$$\rho = x + r$$
$$s = r\varphi \tag{15}$$

Equation 14 may be transformed to:

$$\frac{\partial^2 E_y}{\partial s^2} + (1+cx)^2 \frac{\partial^2 E_y}{\partial x^2} + c(1+cx)\frac{\partial E_y}{\partial x} + (1+cx)^2 k_0^2 n^2(x) E_y = 0 \tag{16}$$

where the constant $c = 1/r$ represents the waveguide curvature. Note that it is easy to see how equation 16 reduces to the scalar wave equation for a straight waveguide when $c=0$. There are some advantages using equation 16. Firstly, the computational window can be restricted because the centre is along the path of the waveguide. Secondly, the index profiles need not be altered as the radius of curvature changes, in contrast to the other methods which use the modified index profile [15]. To solve equation 16 by the MoL, the equation is now discretised using the finite difference operator, by putting:

$$\frac{\partial^2 E_y}{\partial x^2} \approx \frac{E_{i+1} - 2E_i + E_{i-1}}{(\Delta x)^2} \tag{17}$$

and:

$$\frac{\partial E_y}{\partial x} \approx \frac{E_{i+1} - E_{i-1}}{2\Delta x} \tag{18}$$

If this is done, equation 16 can be written in matrix form as:

$$\frac{d^2 \vec{E}}{ds^2} + \vec{Q}\vec{E} = 0 \tag{19}$$

where $\vec{E}$ = $[E_1, E_2, E_3, ..., E_N]^t$ is a column vector containing discretised values of the field $E_y(x)$, at the points $x_1, x_2, ... x_N$, and $\vec{Q}$ is a tri-diagonal matrix defined by :

$$\vec{Q}^2 = \frac{1}{(\Delta x)^2}\begin{bmatrix} -2(1+cx_1)^2 & (1+cx_1)^2 & 0 & 0 \\ (1+cx_2)^2 & -2(1+cx_2)^2 & (1+cx_2)^2 & 0 \\ .. & .. & .. & .. \\ 0 & 0 & (1+cx_N)^2 & -2(1+cx_N)^2 \end{bmatrix} + \tag{20}$$

$$\frac{1}{2\Delta x}\begin{bmatrix} 0 & c(1+cx_1) & 0 & 0 \\ -c(1+cx_2) & 0 & c(1+cx_2) & 0 \\ .. & .. & .. & .. \\ 0 & 0 & -c(1+cx_N) & 0 \end{bmatrix} + k_0\begin{bmatrix} (1+cx_1)^2 n^2 & 0 & 0 & 0 \\ 0 & (1+cx_2)^2 n^2 & 0 & 0 \\ .. & .. & .. & .. \\ 0 & 0 & 0 & (1+cx_N)^2 n^2 \end{bmatrix}$$

Assuming that there is no back-reflection, the general solution for constant matrix elements has the form:

$$\vec{E} = \vec{T} e^{-j\vec{\beta}s} \vec{T}^{-1} \vec{E}_{inp} \tag{21}$$

where $\vec{T}$ is a matrix containing the eigenvectors of $\vec{Q}$ arranged in columns, $\vec{\beta}$ is a diagonal matrix containing the eigenvalues of $\vec{Q}$, and $\vec{E}_{inp}$ is the input field vector. One of the most important parameters associated with the waveguide is the fractional power that remains in the core at point z. This power is approximately given by the overlap integral:

$$P(z) = \left| \int_{-\infty}^{\infty} E(x,0)E(x,z)dx \right|^2 \tag{22}$$

where $E(x,0)$ is the input field and $E(x,z)$ is the field at point z.

2.3. The Absorbing Boundary Condition

To calculate the modal field of the curved waveguide, it is necessary to restrict the extent of the computational window. Once again, this is done using absorbing boundary conditions. Derivation of appropriate boundary conditions in polar co-ordinate is generally rather complicated [16]. In the calculation described here, we have adopted a simpler approach, applying a straight guide boundary condition to the curved waveguide equation, by using the assumption that the radius of curvature is large enough that the mode inside the bend is similar to that of straight guide.

The absorbing boundary condition is inserted into the edge of the matrix components of equation 20 [16]. In this case, we have used the more effective third-order absorbing boundary condition, where the radical is approximated by:

$$\sqrt{1+S^2} \approx \frac{p_0 + p_2 S^2}{q_0 + q_2 S^2} \tag{23}$$

Differences in the choice of the coefficients, p and q, produces different families of absorbing boundary conditions. These result in differences in the angle of exact absorption of the incoming wave by the absorbing boundary layer. Table 1 shows a list of the coefficient values and absorption angles of the approximations that are most commonly used. Here, we have used the L_∞ type of approximation.

Table 1. Coefficients for different third-order absorbing boundary conditions, after reference [4.16]

Type of approximation	p_0	p_2	q_2	angle of exact absorption (^{o})
Pade'	1.0000	-0.7500	-0.2500	0.0
Chebyshev L^∞	0.9997	-0.8086	-0.3165	11.7, 31.9, 43.5
Chebyshev points	0.9965	-0.9129	-0.4725	15.0, 45.0, 75.0
Least square (L_2)	0.9925	-0.9223	-0.5108	18.4, 51.3, 76.6
Chebyshev-Pade' (C-P)	0.9903	-0.9431	-0.5556	18.4, 53.1, 81.2
Newman points	1.0000	-1.0000	0.6697	0.0, 60.5, 90.0
Chebyshev L_∞	0.9565	-0.9435	0.7038	26.9, 66.6, 87.0

q_0 = 1.0000 for each approximation

3. Results and Analysis

To get a better understanding on how the guided mode evolution during its propagation inside curved waveguides; we have used two methods, i.e. an analytical theory that is assumed to be the right approach and the method of lines. In both calculations parameters of a waveguide bends with a radius 5000 μm through an angle of 45° with different refractive index

changes have been used. Figure 3 shows the variation of C_2 calculated using equation 4 with wavelength for different values of Δn, i.e. for different degrees of waveguide confinement. These results show that C_2 increases as the confinement becomes higher and also that C_2 values generally decrease slowly at long wavelengths.
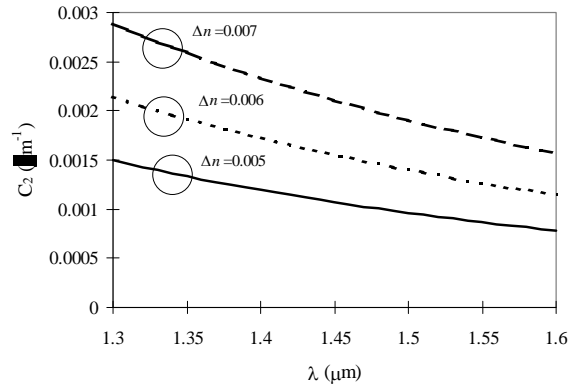

Figure 3. Variation of the parameter C_2 with wavelength, for different values of Δn as predicted by equation 4

Figure 4 (a) and (b) show a comparison of the C_1 and the C_2 values as a function of waveguide width, calculated by Marcatili's approximation of equation 4 and 5; Lee's approximation of equation 10 and 11; and Marcuse's approximation of equation 12 and 13 respectively. Here, the parameters of n_1=1.463, n_2=1458, λ=1.525 μm, with h varying from 4 μm to 7 μm, have been used.
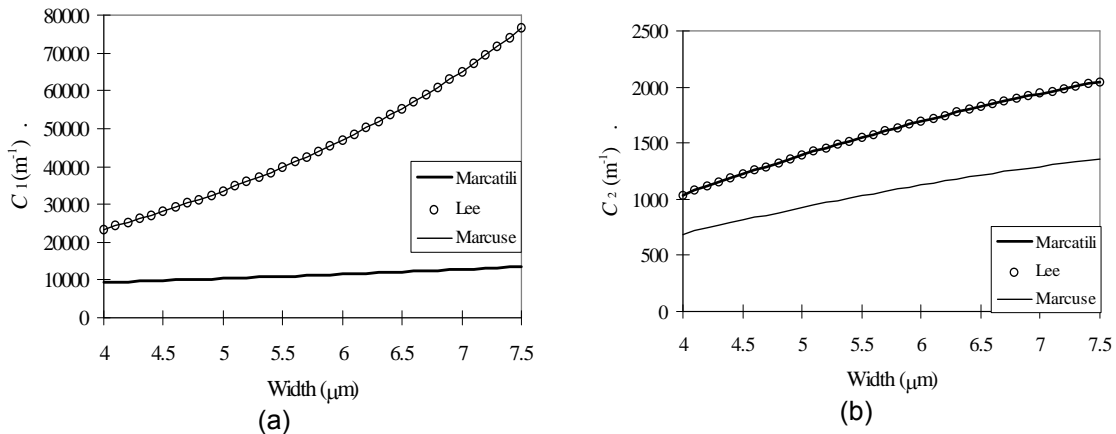

Figure 4. A comparison of different approximations for (a) the C_1 value, and (b) the C_2 value

Figure 4 (a) shows that the C_1 coefficients of Lee's and Marcuse's expression are in a good agreement. However, Marcatili's equation gives much lower value. This might well be because of the different approaches used to derive the C_1 coefficient. The Marcatili approximation is obtained from the complex solution of the eigenvalue equation of the waveguide bend, while both Lee and Marcuse use a different approximation based on the local rate of power radiation from the bend. Furthermore, for the C_2 coefficient, Lee's and Marcatili's approximations give a good agreement, while Marcuse's approach gives apparently incorrect values. It can be concluded that Lee's expression is the most likely to be correct. This assumption will be validated later by comparison with the rigorous method of lines.

To illustrate the way in which the guided mode evolves in a curved waveguide, we first compare the input and output mode shapes obtained after travelling round a bend of radius 5000 μm through an angle of 45°. Figure 5 (a) shows results obtained for a guide of core index 1.464, cladding index 1.458 and width 5 μm at a wavelength of 1.525 μm, while Figure 5 (b) shows results for a similar but less strongly confining guide which has a core index of 1.463. The calculations have been done by using the MOL scheme.
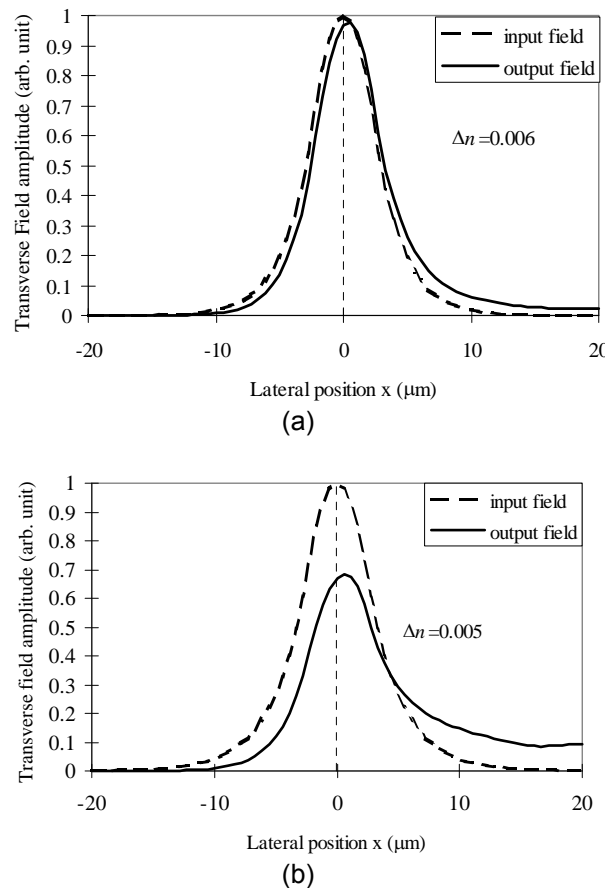

Figure 5. Input and output field distribution of the fundamental mode after travelling around a waveguide bend of radius 5000 μm through an angle of 45⁰. (a) Δn = 0.006, (b) Δn = 0.005

Figure 5 demonstrates that the output field profile of the mode generally extends into the cladding and its peak is reduced, so that it is gradually radiating power. The amount of the power loss depends on the degree of confinement. For example, in Figure 5(a), the output field extends into the cladding only to a very limited extent, and the input and the output field shapes are very similar. However, in Figure 5(b) the output field extends much further into the cladding due to the reduction in confinement. The degree of asymmetry also increases considerably as the confinement is reduced.

We now use the results of the method of lines calculation to estimate an effective attenuation coefficient along a uniformly curved waveguide. This can be done by using equation 1, where the $\dfrac{dP(s)}{ds}$ values are found by evaluating the difference in the integrated optical power across the mode in the computational area between two adjacent axial propagation steps. Figure 6 shows the attenuation coefficient found in this way as a function of bending angle φ, for the parameters Δn=0.005, 0.006, and 0.007, n_2=1.458, λ =1.525 μm, h=5 μm, and r=5000 μm.
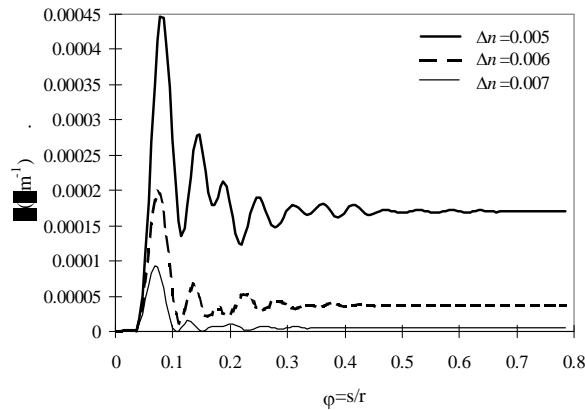
Figure 6. Attenuation coefficient as a function of the bending angle φ, for a different degrees of confinement

In each case, the value of α is not constant, but rises gradually from zero at the start of the bend and settles to a steady-state value only after some rapid fluctuations. In early analyses, the fluctuations have been associated with transition loss [17-18]. However, recently it was demonstrated that they are merely a mathematical artefact which is inherent in numerical modelling of bends using beam propagation methods, and the steady-state value is an accurate estimate of the attenuation coefficient after the mode has settled to its final lateral position.

A comparison of the attenuation coefficients predicted by simple theory and the MoL (at large axial distance) is shown in Figure 8. In the analytical approximations, the C_1 and the C_2 coefficients needed to find the α values have been calculated by using each of the three approximations.
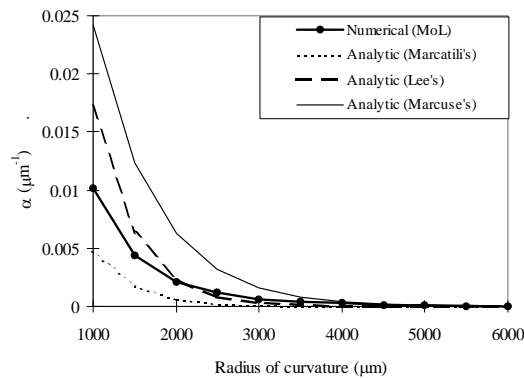

Figure 8. A comparison of the attenuation coefficients obtained from the MoL and from the three different analytical expressions

Figure 8 demonstrates that good agreement is obtained between the analytical form for the loss coefficient based on Lee's expression and the MoL calculation. A slight difference, however, occurs at a small radius. In contrast, Marcatili's formulation predicts a very low value of α when compared to Lee's approximation and the MoL calculation, while Marcuse's formulation predicts much higher values.

The residual discrepancies between the predictions of Lee's theory and the MoL may be explained as follows. In the MoL, the calculation results are highly dependent on a proper choice of absorbing boundary condition at the edge of the computational windows, so that un-suitable conditions give rise to significant reflection back into the computational window and hence lower apparent loss. A similar effect also appears in another numerical scheme [19].

4. Conclusion

We have investigated different analytic approximations to the local loss coefficient in waveguide bends based on constant radius of curvature, and have uncovered disagreement between several previously published analytical expressions. To verify the accuracy of the attenuation coefficient on several publish analytical expression, we have used the beam propagation algorithm based on the method of lines in polar co-ordinate. We have found reasonable agreement with the analytic approximation to the local loss coefficient based on Lee's approach. This agreement might be used to extend the calculation of loss in waveguide bends structure in modelling continuously-varying S-bends waveguides using cascaded section method. Residual disagreement is ascribed mainly to the moderate performance of the absorbing boundary conditions used to limit the range of the calculation window.

References

[1] BE Little, ST Chu, HA Haus, J Foresi, JP Laine. Microring resonator channel dropping filters. *J. Lightwave Technol.* 1997; 15: 998-1005.
[2] M Zirngibl, CH Joyner, LW Stulz, T Gaiffe, C Dragone. Polarization independent 8 × 8 waveguide grating multiplexers on In P. *Electron. Lett.* 1993; 29: 201-202.
[3] RR Hayes, D Yap. GaAs spiral optical waveguides for delay-line applications. *J. Lightwave Technol.* 1993; 11: 523-528.
[4] X Jiang, W Qi, H Zhang, Y Tang, Y Hao, J Yang, M Wang. Loss crosstalk 1 × 2 thermooptic digital optical switch with integrated S-bend attenuator. *IEEE Photon. Technol. Lett.* 2006; 18: 610-612.
[5] F Ladouceur, JD Love. Silica-based buried channel waveguides and devices. Chapman & Hall. London. 1996.
[6] WP Huang. Methods for modeling and simulation of guided-wave optoelectronic devices: part I: modes and couplings. EMW Publishing, Cambridge, Massachusetts, 1995.
[7] SM Saad. Review of numerical methods for the analysis of arbitrarily-shaped microwave and optical dielectric waveguides. *IEEE Trans. on Microwave Theory and Tech.* 1985; MTT-33: 894-899.
[8] T Itoh. Numerical techniques for microwave and millimeter-wave passive structures. John Wiley & Sons. New York. 1989.
[9] U Rogge, R Pregla. Method of lines for the analysis of dielectric waveguides. *IEEE J.Lightwave Technol.* 1993; LT-11: 2015-2020.
[10] EAJ Marcatili. Bends in optical dielectric guides. *Bell Syst. Tech. J.* 1969; 48: 2103-2132.
[11] WJ Minford, SK Korotky, RD Alferness. Low-loss Ti:LiNbO$_3$ waveguide bends at =1.3 m. *IEEE J. Quantum Electron.* 1982; QE-18: 1802-1806.
[12] DL Lee. Electromagnetic principles of integrated optics. John Wiley & sons. New York. 1986.
[13] D Marcuse. Length optimisation of an S-shaped transition between offset optical waveguides. *Appl. Opt.* 1978; 17: 763-768.
[14] D Marcuse. Bending losses of the asymmetric slab waveguide. *Bell Syst. Tech. J.* 1971; 50: 2551-2563.
[15] SJ Garth. Mode behaviour on bent planar dielectric waveguides. *IEE Proc. Optoelectron.* 1995; 142: 115-120.
[16] TG Moore, JG Blaschak, A Taflove, GA Kriegsmann. Theory and application of radiation boundary operators. *IEEE Trans. Antenna and Prop.* 1988; 36: 1797-1812.
[17] J Yamauchi, S Kikuchi, T Hirooka, M Nakano. Beam propagation analysis of bent step-index slab waveguide. *Elect. Lett.* 1990; 26: 822-824.
[18] M Rivera. Lowest-order mode transmission in multimode dielectric S-bends. *Opt. Quantum Electron.* 1997; 29: 323-333.
[19] J Saijonmaa, D Yevick. Beam-propagation analysis of loss in bent optical waveguides and fibers. *J. Opt. Soc. Amer.* 1983; 73: 1785-1791.